Investigation of the Use of Acceleration Estimates by Endgame Guidance Laws

Douglas P. Looze*
University of Massachusetts, Amherst, Massachusetts
and
John Y. Hsu,† and Daniel Grunberg‡
ALPHATECH, Inc., Burlington, Massachusetts

The objective of the work described in this paper is to investigate the use of target acceleration by endgame guidance laws. The approach used is based on a covariance simulation that bounds the error covariance of the estimated states with the Cramer-Rao lower bound of the system. The use of the Cramer-Rao lower bound allows the guidance law performance to be evaluated independently of specific filter designs, while the use of a covariance simulation minimizes the need for expensive and time-consuming Monte-Carlo simulations. Together, the Cramer-Rao lower bound and covariance simulation constitute an efficient analysis tool for investigating tradeoffs and fundamental performance limitations in endgame engagements. The Cramer-Rao lower bound covariance simulation is developed for an endgame engagement system. The analysis capabilities of the Cramer-Rao lower bound simulation are demonstrated by an application to an endgame engagement involving a model of a bank-to-turn missile.

Nomenclature

$A(p,q,r)$ = quaternion dynamics matrix
A^T = transpose of the matrix A
a_{cB} = commanded acceleration in missile body coordinates
a_c = commanded acceleration in inertial coordinates
a_{nc} = commanded normal acceleration
a_{tB} = target acceleration in target body coordinates
a_t = target acceleration in inertial coordinates
a_{ti} = target acceleration changes in target body coordinates
a_{yc} = commanded lateral acceleration
c_D = coefficient of drag
d = relative position vector at the final time
d_m = average miss distance
$E\{\ \}$ = expected value operator
e = quaternion vector
F = linearized dynamics matrix
f = nonlinear system dynamics
f_{cl} = nonlinear closed-loop dynamics (with guidance commands)
g = nonlinear guidance law
H = linearized measurement matrix
h = nonlinear measurement function
J = Fisher information matrix
K_g = guidance gain
K = Kalman gain
K^T = guidance law acceleration gain
L_{IB} = rotation matrix
P = predicted error covariance
$\bar{P}$ = updated error covariance
P_m = projection onto the plane of the miss vector and orthogonal to the velocity vector
p = roll rate
p_c = commanded roll rate
q = pitch rate
R = measurement noise spectral density
$R_z(\psi)$ = single-axis rotation around the subscripted axis by the angular argument
r = yaw rate
$S[\mu,\sigma]$ = random input describing function model of the saturation element
T = missile acceleration profile
t_{go} = time-to-go
t_{mi} = times of acceleration change
$\text{trace}\{\cdot\}$ = sum of the diagonal elements of the matrix argument
u = input or guidance vector
u^0 = nominal guidance commands
v = white Gaussian noise vector
v_m = velocity of the missile in inertial coordinates
v_t = target velocity in inertial coordinates
x^b = relative position vector of the target to the missile in body coordinate system
x = state vector
x^0 = nominal trajectory
x_t = target position vector relative to missile in the inertial coordinate system
z = measurement vector
$\underline{\Gamma}$ = linearized feedthrough of the measurement for the augmented system
Γ = linearized feedthrough of the state estimate to the state
$\delta(t)$ = Dirac impulse distribution
δ_{kl} = Kronecker pulse function
δu = error between the true guidance commands and the nominal guidance commands
$\delta\hat{x}$ = state estimation error
δx = error between the true state and the nominal state
θ = elevation angle
θ_{LOS} = line of sight elevation angle
λ = parameter describing the bandwidth of the target maneuver
ρ = range of target to missile
$\dot{\rho}$ = range rate to target
σ_{anc} = standard deviation of the commanded normal acceleration
σ_{ayc} = standard deviation of the commanded lateral acceleration

Received Feb. 26, 1988; revision received Aug. 8, 1988.

*Associate Professor, Department of Electrical and Computer Engineering.
†Technical Staff Member. Member AIAA.
‡Consultant.

Σ^a = covariance of the augmented state
Σ = covariance of the state
Σ^{12} = cross-covariance of the state and state estimate
σ_m = projected miss covariance
σ_{mf} = miss covariance
σ_{pc} = standard deviation of the commanded roll rate
ϕ = Euler bank angle
Φ = linearized closed-loop dynamics
$\underline{\Phi}$ = linearized dynamics of the augmented state
v_m = magnitude of the missile velocity
χ = augmented state (engagement state and estimator state)
ψ = azimuth angle
ψ_{LOS} = line of sight azimuth angle
ψ_v = azimuth angle describing the rotation of the inertial coordinate system to the target body coordinate system
ω_ϕ = roll rate channel bandwidth
ω_θ = pitch rate channel bandwidth
ω_ψ = yaw rate channel bandwidth
$\partial/\partial x$ = partial derivative with respect to the argument x
$\Re^n$ = n dimensional space of real-valued vectors

I. Introduction

PREDICTED improvements of target acceleration capabilities in air-to-air missile engagements threaten to seriously degrade the performance of current operational guidance laws. Several suggested modifications to popular guidance laws[1-4] and recent developments of optimal guidance laws[5-9] offer potential performance improvements by incorporating estimates of target acceleration in the formulation of the guidance law. However, none of these modifications have yet demonstrated the promised performance improvements under fully realistic conditions.

There are several possible explanations for the disparity between the theoretical development and the practical implementation of guidance laws that use target acceleration. The first and most pessimistic explanation is that target acceleration cannot be detected and estimated quickly or accurately enough for beneficial use by guidance laws from available measurements. A second explanation is that although sufficiently accurate detection and estimation are possible, current estimation algorithm designs, such as the generalized likelihood ratio (GLR) algorithm,[9] have not yet achieved this performance. Third, recent approaches to guidance law design that use target acceleration may be sensitive to acceleration estimate errors such as delayed detection and/or inaccurately estimated magnitudes. In addition, the more complicated guidance law structure used to take advantage of acceleration information may suffer from sensitivities to other measurement or model errors that do not significantly affect current operational laws.

These explanations can be grouped into three fundamental issues relating to estimator and guidance law performance in an air-to-air missile engagement: the ability to estimate target acceleration from available sensor measurements, the ability of current estimation procedures to achieve ideal performance, and the ability of the guidance law designs to cope with estimator uncertainty and sensor and model errors. This paper describes a nonlinear covariance simulation that provides useful insight into these issues.

The covariance simulation employs the Cramer-Rao lower bound to provide an estimate of the best possible state-estimator performance. The Cramer-Rao lower bound approach possesses several advantages over implementing specific estimator designs. By avoiding specific estimator implementations, the simulation allows a designer to separate the issues of estimator and guidance law performance and to easily isolate problems into the guidance law or estimator designs. Individual guidance law designs can be more rapidly evaluated in terms of their ideal performance due to the simplification of the simulation. By estimating the best possible estimator performance, the Cramer-Rao lower bound approach can be used to determine whether the measurements that are available to the state estimator contain sufficient information to be able to detect and estimate target maneuvers, and whether specific estimator designs are efficiently using the information.

The nonlinear covariance analysis provides a computation of the mean and covariance of the engagement state that takes into account the dominant error sources and nonlinearities of the engagement. The simulation can implement differentiable nonlinear models with as much fidelity as required to represent the measurements, dynamics, or guidance law. Other significant nondifferentiable nonlinearities can be implemented in the simulation via random-input describing functions.[10] Currently, random-input describing functions are used to model missile saturation nonlinearities in the engagement model.

The usefulness of the Cramer-Rao lower bound covariance simulation is demonstrated through the analysis of an endgame engagement using a bank-to-turn missile model and a maneuvering target. The engagement scenario is based on the scenario studied in Ref. 11. The application of the Cramer-Rao lower bound simulation to this scenario yields additional insight that is not easily obtained from the Monte-Carlo simulations presented in Ref. 11. Specifically, the Cramer-Rao lower bound demonstrates that the ability to estimate acceleration is not a limiting factor in this engagement for two reasons:

1) There is sufficient information available from the measurements to estimate the target acceleration quickly and accurately.

2) The target maneuver does not significantly affect the engagement geometry or guidance law.

The use of the Cramer-Rao lower bound covariance simulation allows the analysis to isolate the effects of individual phenomena on the guidance law performance. As a result, it is relatively easy to identify factors that are significant in the estimation of target acceleration or that impact the guidance law performance.

The remainder of this paper describes the Cramer-Rao lower bound covariance simulation and its application to the analysis of endgame engagements. The paper is organized as follows. Section II describes the Cramer-Rao lower bound and its use in the nonlinear covariance simulation. The application of the Cramer-Rao lower bound simulation to an endgame engagement model is presented in Sec. III. Section IV presents and analyzes the results of the Cramer-Rao lower bound simulation experiments. The paper is concluded in Sec. V.

II. Nonlinear Covariance Simulation Using the Cramer-Rao Lower Bound

A. Cramer-Rao Lower Bound Analysis

The system is assumed to be modeled as a nonlinear discrete-time system with stochastic measurements:

$$x_{k+1} = f(x_k, u_k) \tag{1}$$

$$z_k = h(x_k) + v_k \tag{2}$$

where $x_k \in \Re^n$ is the state vector, $u_k \in \Re^m$ is the input or guidance vector, $z_k \in \Re^p$ is the measurement vector, and where $v_k \in \Re^p$ is a white Gaussian noise vector with covariance

$$E\{v_k v_\ell^T\} = R_k \delta_{k\ell} \tag{3}$$

Let $\hat{x}_k \in \Re^n$ be the state estimate produced by any unbiased estimator of the state x_k (i.e., $E\{\hat{x}_k - x_k\} = 0$) that uses the measurements $\{z_j\}_{j=1}^k$. For the purpose of propagating the covariance of the state, the guidance law is assumed to be a function of the state-estimate vector $\hat{x}$ (using measurements up to and including z_k):

$$u_k = g(\hat{x}_k) \tag{4}$$

For the purpose of computing the Cramer-Rao lower bound of the estimator error covariance and for computing the nominal state trajectory, the guidance law is assumed to be a function of the state vector

$$\mathbf{u}_k = g(x_k) \tag{5}$$

The difference in these two assumptions requires some discussion. In general, a combination of a guidance law and a state estimator will be implemented with the guidance law being a function of the state estimates provided by the estimator. Thus, Eq. (4) is a realistic model of the guidance law implementation, while Eq. (5) is an approximation of the actual implementation. Although the principal motivation for this approximation is that it is needed to make the computation of the Cramer-Rao lower bound feasible, the approximation yields an accurate approximation of the true Cramer-Rao lower bound whenever the state-estimate error that is fed back through the guidance law via Eq. (4) is not a dominant source of error for the state estimator. Since a primary objective of the guidance law design should be to mitigate estimation errors, the source of estimation errors originating from the feedback loop will be significantly less than the errors induced directly by the measurements. Hence, the assumption that the guidance law will in general depend directly on the state is reasonable for the computation of the Cramer-Rao lower bound estimate of the state-estimation error covariance.

The Cramer-Rao lower bound provides a lower bound on the error covariance that can be achieved by any unbiased estimate for a nonlinear stochastic system in terms of the Fisher information matrix. For systems that have no process noise (i.e., the state equation is deterministic), the Fisher information matrix can be computed easily. The engagement model given by Eqs. (1), (2), and (5) satisfies this requirement. Hence, the error covariance along the nominal deterministic solution x_k^0 to Eqs. (1) and (5)

$$P_k = E\{(\hat{x}_k - x_k)\,(\hat{x}_k - x_k)^T\} \tag{6}$$

is bounded by

$$P_k \geq J_k^{-1} \tag{7}$$

where J_k is the Fisher information matrix.[12]

The Fisher information matrix along the nominal trajectory is computed using the linear propagation equation[13]:

$$J_{k+1} = F_k^{-T} J_k F_k^{-1} + H_{k+1}^T R_{k+1}^{-1} H_{k+1} \tag{8}$$

where R_k is the measurement noise matrix (3), and F_k and H_k are the linearized dynamics and measurement matrices along the nominal trajectory:

$$F_k = \left[\frac{\partial}{\partial x} f(x,u) + \frac{\partial}{\partial u} f(x,u)\,\frac{\partial}{\partial x}\, g(\mathbf{x})\right]_{x = x_k^0,\ u = u_k^0} \tag{9}$$

$$H_k = \left[\frac{\partial}{\partial x}\, h(x)\right]_{x = x_k^0} \tag{10}$$

The Cramer-Rao lower bound can be computed as the inverse of the covariance matrix of the linearized system. Let $f_{cl}(\cdot)$ be defined as the closed-loop state dynamics:

$$f_{cl}(x) \equiv f[x, g(x)] \tag{11}$$

The state estimate $\hat{x}_k$ propagates by the equation

$$\hat{x}_{k+1} = f_{cl}(\hat{x}_k) + K_{k+1}\{h(x_{k+1}^0) + v_{k+1} - h[f_{cl}(\hat{x}_k)]\} \tag{12}$$

where K_k is the Kalman gain. Define the state-estimation error

$$\delta\hat{x}_k = \hat{x}_k - x_k \tag{13}$$

Linearizing Eq. (12) around the nominal trajectory x_k^0 yields the linearized Kalman filter propagation equation:

$$\delta\hat{x}_{k+1} = (I - K_{k+1}H_{k+1})F_k\delta\hat{x}_k + K_{k+1}v_{k+1} \tag{14}$$

where F_k and H_k are the linearized state and measurement matrices given by Eqs. (9) and (10). The linearized Kalman gain is given by

$$K_k = \underline{P}_k H_k^T\,[H_k \underline{P}_k H_k^T + R_k]^{-1} \tag{15}$$

where the predicted error covariance $\underline{P}_k$ and the updated error covariance P_k are given by

$$\underline{P}_{k+1} = F_k P_k F_k^T \tag{16}$$

$$P_{k+1} = [I - K_{k+1}H_{k+1}]P_{k+1} \tag{17}$$

Alternatively, the inverse of the covariance matrix can be propagated. Substituting Eq. (15) in Eq. (17) and inverting yields

$$P_{k+1}^{-1} = \underline{P}_{k+1}^{-1}\{I - P_{k+1}H_{k+1}^T[H_{k+1}\underline{P}_{k+1}H_{k+1}^T + R_{k+1}]^{-1}H_{k+1}\underline{P}_{k+1}\}^{-1} \tag{18}$$

A standard matrix identity[14] can be applied to simplify the right side of Eq. (18):

$$P_{k+1}^{-1} = \underline{P}_{k+1} + H_{k+1}^T R_{k+1}^{-1} H_{k+1} \tag{19}$$

Finally, substituting Eq. (16) into Eq. (19) yields the propagation for P_{k+1}^{-1}:

$$P_{k+1}^{-1} = F_k^{-T} P_k^{-1} F_k^{-1} + H_{k+1}^T R_{k+1}^{-1} H_{k+1} \tag{20}$$

Equation (20) is identical to the Fisher information matrix propagation Eq. (8) with P_k^{-1} replacing J_k. Thus, the Cramer-Rao lower bound is equal to the estimation error covariance matrix obtained from a linearized (about the nominal state x_k^0) Kalman filter in the absence of process noise. That is, the Fisher information matrix is

$$J_k = P_k^{-1} \tag{21}$$

Since the actual implementation of the guidance law uses the state estimate [Eq. (4)] rather than the true state [Eq. (5)] as assumed by the Cramer-Rao lower bound presentation in Eqs. (6–10), the lower bound [Eq. (6)] may be violated in some systems. However, most well-behaved systems will see an increase in the covariance of the state estimator due to the additional noise that is introduced to the evolution of the state by the guidance law. In any case, as was noted previously, the relative change in the covariance due to errors in the state estimate is likely to be small for reasonable guidance law designs.

B. Nonlinear Covariance Analysis

The Cramer-Rao lower bound described in Eqs. (6–9) is used to estimate the ideal error covariance of a state estimate. One of the primary objectives of this paper is to develop a tool to evaluate the effects of the state-estimate error and other error sources (such as unmodeled dynamics, target acceleration, parameter variations, nonlinearities, and sensor accuracies) on an engagement. The criteria that will be used to evaluate these effects on engagements are the deterministic miss distance and the average miss distance. Good approximations of these two quantities can be computed from the mean (i.e., the deterministic propagation) of the engagement states and from the covariance of the engagement states. The mean and covariance of the engagement state will be computed using a nonlinear covariance simulation. The nonlinear co-

variance simulation employs a linearized covariance propagation combined with the use of describing functions to incorporate the effects of important nonlinearities. This subsection will develop the nonlinear covariance propagation equations for the state x_k.

Given the state propagation equation (1), the measurement equation (2), measurement noise statistics [Eq. (3)], the guidance law implementation [Eq. (4)], and the error covariance of the state estimate, the objective of the nonlinear covariance simulation is to compute the covariance of the state:

$$\Sigma_k = E\{(x_k - x_k^0)(x_k - x_k^0)^T\} \tag{22}$$

It will be assumed that the state model [Eq. (1)] includes any random input describing functions that are used to represent nonlinearities in the engagement system. It will also be assumed that the state x_k is perturbed from its nominal trajectory by an amount δx_k, and the acceleration command u_k is perturbed by an amount δu_k:

$$\delta x_k = x_k - x_k^0 \tag{23}$$

$$\delta u_k = u_k - u_k^0 \tag{24}$$

where u_k^0 is the nominal acceleration command. The source of the perturbation errors is the state estimation error $\delta\hat{x}_k$ given by Eq. (13). Note that the actual covariance of the state-estimation error is the error covariance P_k, which is bounded by the Cramer-Rao lower bound J_k^{-1} [Eq. (7)].

The state equation (1) and guidance law can be linearized around the nominal state and nominal acceleration command trajectories and combined to yield the linearized state equation

$$\delta x_{k+1} = \Phi_k \delta x_k + \Gamma_k \delta\hat{x}_k \tag{25}$$

where

$$\Phi_k = \left[\frac{\partial}{\partial x} f(x,u_k^0)\right]_{x=x_k^0} \tag{26}$$

$$\Gamma_k = \left[\frac{\partial}{\partial u} f(x,u)\,\frac{\partial}{\partial x} g(x)\right]_{x=x_k^0,\,u=u_k^0} \tag{27}$$

Since δx_k and $\delta\hat{x}_k$ are correlated, their respective covariances must be propagated simultaneously. Thus, we define the augmented state

$$\chi_k = [\delta x_k^T \;\delta\hat{x}_k^T]^T \tag{28}$$

where $\delta\hat{x}_k$ represents the linearized state estimator error defined by Eq. (13). In general the cross correlation between the true state and any specific state estimator will depend on the estimation algorithm that is used. However, the use of the linearized state-estimation error is consistent with the philosophy of the Cramer-Rao lower bound approach, and will produce an accurate estimate whenever the Cramer-Rao lower bound is accurate.

The augmented state defined by Eq. (27) propagates according to the linearized equation

$$\chi_{k+1} = \underline{\Phi}_k \chi_k + \underline{\Gamma}_k v_{k+1} \tag{29}$$

where

$$\underline{\Phi}_k = \begin{bmatrix} \Phi_k & \Gamma_k \\ 0 & (I - K_{k+1}H_{k+1})F_k \end{bmatrix} \tag{30}$$

$$\underline{\Gamma}_k = \begin{bmatrix} 0 \\ K_{k+1} \end{bmatrix} \tag{31}$$

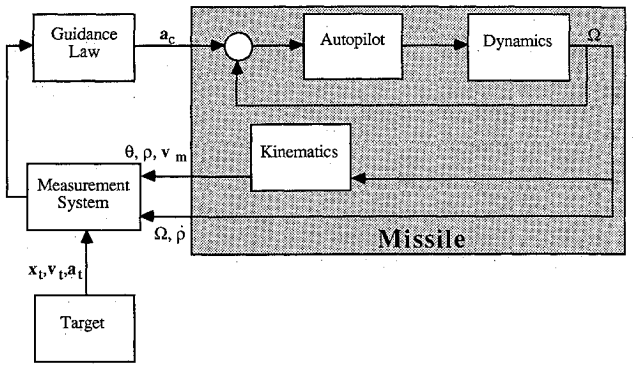

Fig. 1 Components of the endgame model.

To first order [i.e., based on the linearized system (29)] the perturbed augmented state χ_k and the perturbed acceleration commands δu_k have zero mean. Since $E\{\chi_k\} = 0$, the covariance of χ_k is propagated by the discrete Lyapunov equation:

$$\Sigma_{k+1}^a = \underline{\Phi}_k \Sigma_k^a \underline{\Phi}_k^T + \underline{\Gamma}_k R_{k+1} \underline{\Gamma}_k^T \tag{32}$$

where

$$\Sigma_k^a = E\{\chi_k \chi_k^T\} \tag{33}$$

The covariance matrix Σ_k can be partitioned to conform with the partitioning of χ_k [Eq. (28)]:

$$\Sigma_k^a = \begin{bmatrix} \Sigma_k & \Sigma_k^{12} \\ (\Sigma_k^{12})^T & P_k \end{bmatrix} \tag{34}$$

where

$$\Sigma_k^{12} \equiv E\{\delta x_k\, \delta x_k^T\} \tag{35}$$

Note that the desired covariance of the state Σ_k can be obtained from the upper-left partition of the covariance matrix Σ_k^a, whereas the best possible estimator error covariance P_k is given by the lower-left partition of the same covariance matrix. Thus, both the ideal estimator performance and the effects of estimation error on the engagement can be evaluated through the solution of the Lyapunov equation (32).

III. Engagement Model

A. Engagement Dynamics

The endgame engagement model, consisting of the target, the missile, the measurement system or sensors, and the guidance law, is depicted in Fig. 1. The motion of the missile body is determined by the dynamics and kinematics of the missile and by the actions of the autopilot in response to the commands of the guidance system. The missile-body motion and the target motion are sensed by the measurement system, and the measurements are supplied to the guidance law. The guidance law then supplies commanded accelerations and roll rates to the missile-body system.

The formulation of the endgame model will use three reference coordinate systems: a missile-body coordinate system, a target-body coordinate system, and a stationary inertial reference coordinate system. The missile-body coordinate system is a right-hand coordinate system that is aligned with the missile body at all times. Given the Euler bank angle ϕ, elevation angle θ, and azimuth angle ψ, the rotation from the inertial coordinate system to the missile-body coordinate system is specified by the rotation matrix $L_{IB}(\phi,\theta,\psi)$. The target-body coordinate system is a right-hand coordinate system that is aligned with the target body at all times.

The target motion will be represented by a simple three-degree-of-freedom point-mass model with constant mass. In the

inertial coordinate system, let x_t represent the relative position of the target with respect to the missile, let v_t represent the target velocity, and let a_t represent the target acceleration. The model for target acceleration (i.e., the target maneuver) assumes a constant centripetal acceleration in the x-y inertial plane, or a constant linear acceleration in the z inertial plane. Either of these constants can change magnitudes instantaneously a finite number of times. The former model will be used to represent an initially nonmaneuvering target that executes a constant angular velocity, constant radius (circular) turn. The latter model will be used to represent a constant acceleration dive. More detailed models of target maneuvers can be readily implemented.

Since the target will be modeled as a point mass, the target-body coordinate system is defined by the velocity vector together with the assumptions that the target elevation and roll angles are zero. Thus, the rotation of the target-body coordinate system to the inertial coordinate system is determined by the azimuth angle ψ_v. The azimuth angle ψ_v is given in terms of the x and y coordinates of the target velocity:

$$\tan\psi_v = v_{ty}/v_{tx} \tag{36}$$

where the tangent accounts for the quadrant of the velocity vector. The acceleration in inertial coordinates is then

$$a_t = R_z(\psi_v)a_{tB} \tag{37}$$

where $R_z(\psi_v)$ is the single-axis rotation about the z axis by ψ_v.

The target state consists of the vectors x_t, v_t, and a_{tB}, and evolves according to the equations

$$\dot{x}_t = v_t - v_m \tag{38}$$

$$\dot{v}_t = a_t \tag{39}$$

$$\dot{a}_{tB} = \sum_{i=1}^{n_m} a_{ti}\delta(t - t_{mi}) \tag{40}$$

where a_{ti} are the acceleration changes in target body coordinates, t_{mi} are the times of acceleration change, and δ denotes the Dirac impulse distribution.

The closed-loop subsystem consisting of the missile dynamics and kinematics, and the missile autopilot, will be represented using a six-degree-of-freedom model with greatly simplified dynamics. The model is obtained by assuming that the autopilot is designed to decouple each of the rate channels (see Fig. 1) and, consequently, that the response of the autopilot/dynamics loop can be modeled as three independent first-order lags. Although this assumption about the autopilot performance will not be valid for all purposes and should be verified on a case by case basis, it has the advantage of isolating the effects of the engagement geometry from the effects of a nonideal missile. Thus, the fundamental limitations associated with the engagement geometry and ideal missile behavior can be identified.

The commanded body rates are determined from the saturated guidance law commands for normal acceleration a_{nc}, lateral acceleration a_{yc}, and roll rate p_c. The roll rate command is used directly, whereas the pitch rate and yaw rate commands are calculated by dividing the normal and lateral accelerations by the magnitude of the velocity. The latter calculation assumes that the velocity vector is approximately aligned with the body forward axis. Assuming the independent pitch, yaw, and roll rate channels have bandwidths ω_q, ω_ψ, and ω_ϕ, respectively, the model for the evolution of pitch rate q, yaw rate r, and roll rate p is

$$\dot{q} = -\omega_\theta q + \omega_\theta S[a_{nc},\sigma_{anc}]/v_m \tag{41}$$

$$\dot{r} = -\omega_\psi q + \omega_\psi S[a_{yc},\sigma_{ayc}]/v_m \tag{42}$$

$$\dot{p} = -\omega_\phi q + \omega_\phi S[p_c,\sigma_{pc}] \tag{43}$$

$$v_m = \sqrt{v_{mx}^2 + v_{my}^2 + v_{mz}^2} \tag{44}$$

where $S[\mu,\sigma]$ is a random input describing function model of the saturation element, and σ_{anc}, σ_{ayc}, and σ_{pc} are the standard deviations of the commanded normal acceleration, lateral acceleration, and roll rate, respectively. The standard deviations are obtained from the Cramer-Rao lower bound covariance matrix.

The velocity of the missile is assumed to be aligned with the missile body (i.e., the angle of attack and sideslip are assumed to be negligible for computing the velocity vector direction). The evolution of the velocity magnitude is modeled as the sum of an acceleration term determined by the missile acceleration profile $T(t)$, and a drag term that is modeled as being proportional to the missile velocity. Thus, the model for the missile velocity is

$$\dot{v}_m = -c_D v_m + T \tag{45}$$

The velocity vector v_m in the inertial coordinate system is then determined from the Euler angles' relating the inertial coordinate system to the body coordinate system by the equation

$$v_m = v_m L_{IB}(\phi,\theta,\psi)^T n_1 \tag{46}$$

where

$$n_1 = [1 \quad 0 \quad 0]^T$$

The model will use quaternions to integrate the body rates. The evolution of the quaternions is given by a linear differential equation whose coefficients are determined by the body rates

$$\dot{e} = A(p,q,r)e \tag{47}$$

where the 4×4 matrix A is given by

$$A(p,q,r) = \begin{bmatrix} 0 & -p & -q & -r \\ p & 0 & r & -q \\ q & -r & 0 & p \\ r & q & -p & 0 \end{bmatrix} \tag{48}$$

The rotation matrix L_{IB} can be computed from e by the following formulas:

$$L_{IB}(\phi,\theta,\psi) = \begin{bmatrix} e_0^2+e_1^2-e_2^2-e_3^2 & 2(e_1e_2+e_0e_3) & 2(e_1e_3-e_0e_2) \\ 2(e_1e_2-e_0e_3) & e_0^2-e_1^2+e_2^2-e_3^2 & 2(e_2e_3+e_0e_1) \\ 2(e_1e_3+e_0e_2) & 2(e_2e_3-e_0e_1) & e_0^2-e_1^2-e_2^2+e_3^2 \end{bmatrix} \tag{49}$$

where $e = [e_0\ e_1\ e_2\ e_3]^T$.

The model defined by the equations of this section is discretized and implemented in discrete time. The engagement state consists of the relative target position, the target velocity, the target acceleration, the missile velocity, the missile-body rates, and the quaternions for a total of 19 engagement states:

$$x = [x_t^T\ v_t^T\ a_{tB}^T\ v_t^T\ p\ q\ r\ e^T]^T \tag{50}$$

Target acceleration has been included as an engagement state (rather than as a predetermined function) since one of the goals of this paper is to investigate the ability to estimate acceleration in an engagement environment.

B. Measurement Model

Four measurements based on the engagement state vector have been implemented:

$$h(x_k) = [\rho(k)\ \dot{\rho}(k)\ \psi_{LOS}(k)\ \theta_{LOS}(k)]^T \tag{51}$$

where

$\rho(k)$ ≡ range of target to missile

$\dot{\rho}(k)$ ≡ range rate to target

$\psi_{\text{LOS}}(k)$ ≡ line of sight azimuth angle

$\theta_{\text{LOS}}(k)$ ≡ line of sight elevation angle

The range ρ is a straightforward calculation from the target relative position vector:

$$\rho = \sqrt{x_t^T x_t} \tag{52}$$

Range rate is given by the time derivative of Eq. (52). Noting that the time derivative of x_t is determined by Eq. (38), the range rate is

$$\dot{\rho} = \frac{1}{\rho} x_t^T (v_t - v_m) \tag{53}$$

The line-of-sight angles are computed from the relative position vector x^b of the target to the missile in the body axis. The vector x^b is obtained by rotating the relative target position vector into the body coordinate system using the rotation matrix L_{IB}:

$$x^b = L_{IB}(\phi,\theta,\psi) x_t \tag{54}$$

Let $x^b = [x^b y^b z^b]^T$. Then the line-of-sight angles are computed from the trigonometric formulas:

$$\theta_{\text{LOS}} = \tan^{-1}\left[\frac{z^b}{x^b}\right] \tag{55}$$

$$\psi_{LOS} = \tan^{-1}\left[\frac{y^b}{\sqrt{(x^b)^2 + (z^b)^2}}\right] \tag{56}$$

The measurement equation analysis uses the measurements defined by Eqs. (51–56) with additive white noise [see Eqs. (2) and (3)]. The components of the noise vector v_k will be assumed to be uncorrelated, which implies that the covariance matrix R_k is diagonal:

$$R_k = \text{diag}[r_{ii}(k)] \tag{57}$$

The accuracy of the range and range rate measurements is assumed to be time-independent. Consequently, the diagonal elements of the covariance matrix corresponding to these two measurements are constants:

$$r_{11}(k) = r_\rho, \qquad r_{22}(k) = r_{\dot{\rho}} \tag{58}$$

The errors in the remaining measurements involve angular resolutions. These errors will be assumed to be range-dependent, with the standard deviation of the error being inversely proportional to the range (for target sizes small relative to the range). Thus, the error model is

$$r_{ii}(k) = r_{ii0}/\rho(k)^2 \tag{59}$$

C. Advanced Guidance Law Model

The guidance law that will be used to define the lateral and normal acceleration commands is the advanced guidance law developed in Ref. 16. The implementation will follow the discussion in Ref. 11. Specifically, the advanced guidance law[16] is defined in inertial coordinates by the following equation:

$$a_c = \frac{K_g}{t_{\text{go}}^2} x_t + \frac{K_g}{t_{\text{go}}} (v_t - v_m) + K_g K_T a_t \tag{60}$$

where a_c is the commanded acceleration in inertial coordinates, K_g is the guidance gain, and K_T is the acceleration gain defined in terms of the time-to-go t_{go} as

$$K_T = \frac{e^{-\lambda t_{\text{go}}} + \lambda t_{\text{go}} - 1}{(\lambda t_{\text{go}})^2} \tag{61}$$

where λ is a parameter describing the bandwidth of the target maneuver. The time-to-go t_{go} is estimated from the current range and closing speed as

$$t_{\text{go}} = -\rho/\dot{\rho} \tag{62}$$

The computation of the guidance commands [Eq. (60)] requires the target acceleration to be expressed in inertial coordinates. Since the model uses target-body coordinates for the target acceleration model, the target acceleration must be converted to inertial coordinates by Eqs. (36) and (37).

Given the commanded acceleration in inertial coordinates a_c computed from Eqs. (60–62), the commands must be converted to missile-body coordinates a_{cB} to be implemented in Eqs. (41–43):

$$a_{cB} = L_{IB}(\phi,\theta,\psi) a_c \tag{63}$$

Finally, the guidance law defined by Eqs. (60–63) will generally produce a nonzero axial acceleration command. Since the axial command cannot be implemented by the bank-to-turn missile, it will simply be ignored. The resulting lateral and normal commands are defined by

$$a_{cB} = [a_x \; a_{yc} \; a_{nc}]^T \tag{64}$$

The remaining command to be generated is the roll rate command p_c that is implemented as described in Ref. 11. The principal objective of the roll rate command is to align the missile vertical axis with the commanded acceleration vector. Thus, the desired change in roll angle $\Delta\phi_c$ is

$$\Delta\phi_c = \sin^{-1}\left[\frac{a_{nc}}{a_{yc}}\right] \tag{65}$$

which can be approximated as

$$\Delta\phi_c = \frac{a_{nc}}{a_{yc}} \tag{66}$$

The roll rate command is a constant gain times the desired change in roll angle:

$$p_c = K_\phi \Delta\phi_c \tag{67}$$

D. Miss Covariance Calculation

The Cramer-Rao lower bound simulation produces two statistics that describe the final miss distance: the magnitude of the miss distance vector d, and the miss covariance σ_{mf}. The projected magnitude of the miss distance vector at time k is

$$d_k = \|x_t + t_{\text{go}}(v_t - v_m)\| \tag{68}$$

where t_{go} is the estimated time-to-go. The values of d_k are saved for the three most recent time steps. When the simulation is ended, these values are used in a quadratic interpolation algorithm to produce a value for the magnitude of the final miss vector d.

The miss covariance describes the uncertainty of the point of nearest approach of the missile to the target around the miss distance vector. Thus, the uncertainty of motion along the missile velocity vector does not contribute to the miss distance covariance. The projected miss covariance σ_m is computed at each time step of the simulation from the 3×3 submatrix of the state covariance matrix Σ_k corresponding to

the position states. The final miss covariance is computed by interpolating the projected miss covariance computed at the three most recent time samples.

To eliminate the uncertainty along the missile velocity, the miss covariance is computed in the plane of the miss vector and orthogonal to the velocity vector. The projection onto this plane is

$$P_m = I - \frac{(v_t - v_m)(v_t - v_m)^T}{\|v_t - v_m\|^2} \tag{69}$$

The projected miss covariance is then given by the projection of the position uncertainty matrix (i.e., the 3×3 submatrix Σ_p of the state covariance matrix Σ_k corresponding to the position states) using the projection matrix P_m:

$$\sigma_m = \text{trace}\{P_m \Sigma_p P_m^T\} \tag{70}$$

where the function trace $\{\cdot\}$ is the sum of the diagonal elements of the argument. The values of σ_m are saved for the three most recent time steps. When the simulation is ended, these values are used in a quadratic interpolation algorithm to produce a value for the final miss covariance σ_{mf}.

For small values of the magnitude of the miss distance vector, the miss covariance can be used to compute the average (mean) miss distance. Assuming that the distribution of the miss vector around its mean is Gaussian and that the conditional covariance is equal to $(\sigma_{mf}/2)$ in any direction in the miss plane, the average miss distance is given by

$$d_m = \sqrt{\frac{\sigma_{mf}}{\pi}} \tag{71}$$

E. Model Parameter Value Selection

The parameter values for the models described in subsections III.A–III.D were selected to represent the bank-to-turn missile and target that were studied in Ref. 11 as nearly as possible. The parameters that were selected can be found in Ref. 17.

IV. Cramer-Rao Lower-Bound Covariance Simulation Results

A. Engagement Scenarios

A total of 24 engagement scenarios that varied the initial range, target maneuver, and target acceleration information for the guidance law were examined. The nominal initial engagement geometry, illustrated in Fig. 2, corresponds to a 90-deg aspect angle and a 0-deg off-boresight angle. The missile body and inertial coordinate systems are initially aligned, with an initial velocity of 970 ft/s along the x-axis. The nominal initial target position is at a range of 3000 ft along the x-axis, with an initial velocity of 900 ft/s along the y-axis. The initial range was varied from 2000–5000 ft in 1000-ft increments.

Three different information sources were considered for the target acceleration in the guidance law implementation. The nominal implementation models the use of a target acceleration estimate by using the Cramer-Rao lower bound bounds in the propagation of the engagement statistics. The second information source assumes perfect target acceleration estimates. The third information source uses no target acceleration information in the computation of the guidance commands.

Two target maneuvers were also considered. The first maneuver (identical to the maneuver considered in Ref. 11) consists of a constant centripetal acceleration of 288 ft/s^2 (9 g, where g is the acceleration of gravity), constant radius turn toward the missile that begins at the start of the simulation. The second maneuver is a constant 288 ft/s^2 acceleration dive that also begins at the start of the simulation. Although the latter maneuver would result in an unbounded vertical velocity if continued indefinitely, it is a reasonable model for the target motion over the short period of the engagement (less than 3 s for each experiment). A more exhaustive study could include more detailed models of target maneuvers and more realistic target dynamics.

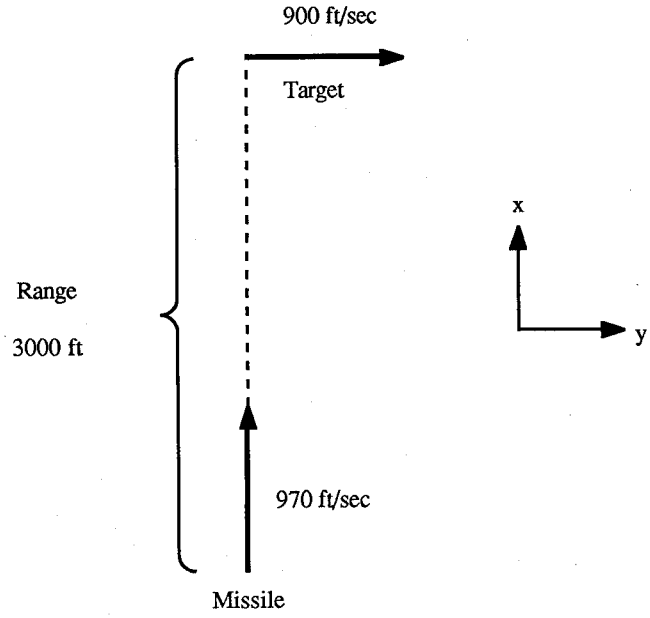

Fig. 2 Initial engagement geometry.

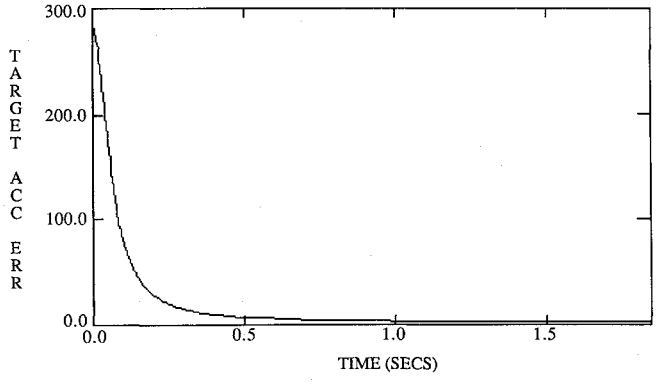

Fig. 3 Cramer-Rao lower bound of the acceleration estimation error vs time, for the turn maneuver.

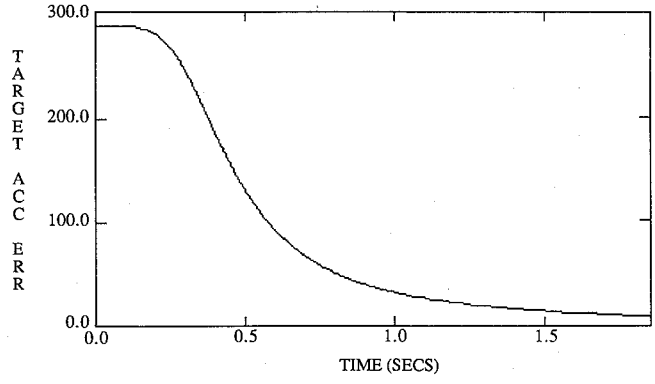

Fig. 4 Cramer-Rao lower bound of the acceleration estimation error vs time, for the dive maneuver.

B. Target Acceleration Estimation for the Nominal Scenario

The square root of the Cramer-Rao lower bound of the error covariance for the target acceleration state in the maneuver direction is shown in Fig. 3 for the turn maneuver and in Fig. 4 for the dive maneuver.

Note that for the turn maneuver most of the error is eliminated within the first 0.3 s of the engagement, and by 0.5 s the standard deviation of the error is less than 10 ft. This error would contribute less than 15 ft/s^2 to the acceleration command, which represents less than 1% of the peak total acceleration command. Consequently, the acceleration estimate error is not likely to be a major factor in the endgame performance.

The reason for the ability to estimate the target acceleration quickly and accurately is that the turn maneuver consists of an acceleration that is almost perfectly aligned with the relative position vector during the entire maneuver. Figure 5 illustrates the relative positions of the target and missile, and the velocity and acceleration vectors at the time of the largest relative lateral position. The component of the target acceleration orthogonal to the relative position vector is only 15.4 ft/s^2. Thus, almost all the effects of the target acceleration are directly observable by the range and range rate measurements, which are relatively accurate.

The speed of response of the acceleration estimate error is considerably slower for the dive maneuver (see Fig. 4). Since this maneuver is initially unobservable through the range and range rate measurements, any information must be accumulated through the line of sight angle measurements. The resolution of the line-of-sight angle measurements is approximately 10 times worse than that of the range and range rate measurements. As a result, the acceleration error takes 1.0 s to be reduced to less than 32 ft/s^2, and the final error is nearly 10 ft/s^2.

C. Guidance Law Performance

For all 24 scenarios, the deterministic miss distance was less than 0.8 ft and less than 8.5% of the miss covariance. Hence, the approximation [Eq. (70)] for the average miss distance can be used to accurately compare the results for the engagement scenarios. The average miss distances are plotted as a function of range for each information source in Figs. 6 and 7. Figure 6 shows the average miss distances for the turn maneuver, and Fig. 7 shows the average miss distances for the dive maneuver.

The most striking feature of the results for the turn maneuver is the lack of any significant dependence on range or acceleration information. This insensitivity is due to two geometric features of the engagement:

1) The engagement is essentially a coplanar engagement once the missile has rolled to align its vertical axis with the target velocity and acceleration vectors.

2) The target acceleration vector is almost perfectly aligned with the relative-position vector between the target and missile (see Fig. 5).

The first feature reduces the insensitivity to range since all the ranges considered allow sufficient time for the missile to complete the roll maneuver (0.5 s) and conduct a majority of the engagement in the missile normal plane. The second feature virtually eliminates the target acceleration as a factor in the engagement. The acceleration directly toward the missile simply serves to reduce the engagement time and expand the inner launch envelope. However, the inner launch envelope for this model is not a factor in the ranges that were studied. Also, only the component of acceleration orthogonal to the missile-body x-axis contributes to the guidance commands. The maximum command due to the target acceleration is 123 ft/s^2, which is less than 6% of the maximum acceleration command. Thus, the presence or absence of acceleration information will not significantly affect the performance of the guidance law.

The results for the dive maneuver exhibit a dependency on both the range and the target acceleration that is consistent with intuition. Since the target acceleration is orthogonal to both the engagement plane and the missile body axis for much of the engagement, it should be expected that better information about the target acceleration and more time (i.e., greater range) to react to the target maneuver would reduce the miss distance. The results of the Cramer-Rao lower bound simulation illustrate the expected effects of acceleration information

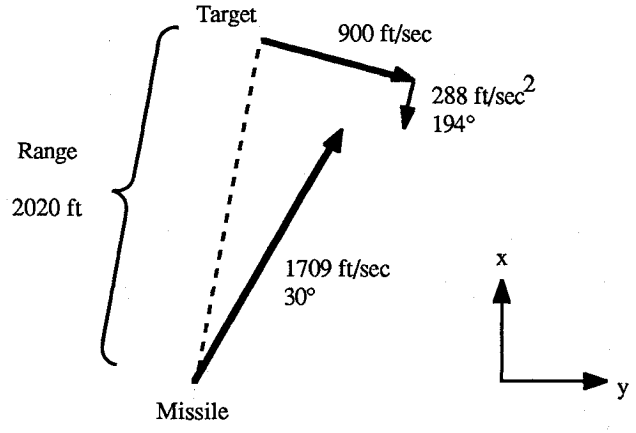

Fig. 5 Engagement geometry for the nominal scenario at 0.74 s.

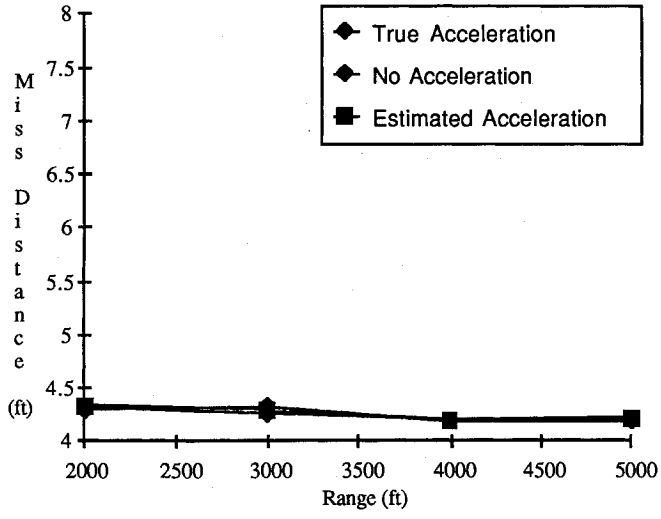

Fig. 6 Expected miss distance for turn maneuver.

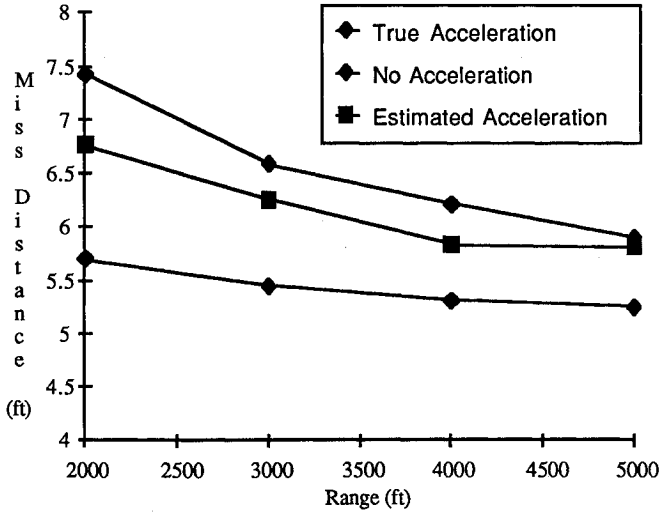

Fig. 7 Expected miss distance for dive maneuver.

and range. Although the absolute difference is relatively small for the ranges examined, the trend to greater differences as the range decreases suggests that the acceleration information might have a significant effect on the inner launch envelope.

V. Conclusions

This paper has presented a nonlinear covariance simulation that uses the Cramer-Rao lower bound, which is useful for analyzing endgame engagements. The simulation was applied to an endgame engagement to investigate 1) fundamental limitations on the ability to estimate target acceleration, and 2) the value of target acceleration estimates to the guidance law performance.

The results illustrate that the Cramer-Rao lower bound simulation is a valuable tool for addressing such fundamental questions concerning guidance law performance. It provides results that are consistent with other reported work, while yielding greater insight into the causes of trends and phenomena that are observed. The simulation reduces the need for expensive and time-consuming Monte Carlo simulations, thereby expediting tradeoff studies and experimental investigations. It also aids the identification of phenomena that limit guidance law performance capabilities both by eliminating the averaging required by Monte-Carlo approaches and by eliminating the dependence of the results on an explicit filter design.

Acknowledgment

This work was supported by the United States Air Force Armament Division under contract number F08635-85-C-0127 at ALPHATECH, Inc.

References

[1]Alexelband, E. I. and Hardy, F. W., "Quasi-Optimum Proportional Navigation," *IEEE Transactions on Automatic Control,* Vol. AC-15, Dec. 1970, pp. 620–626.

[2]Arbenz, K., "Proportional Navigation on Nonstationary Targets," *IEEE Transactions on Aerospace and Electronic Systems,* Vol. AC-15, July 1970, pp. 455–457.

[3]Siouris, G. M., "Comparison Between Proportional and Augmented Proportional Navigation," *Nachrichientechnische Zeitschrift,* July 1974, pp. 278–280.

[4]Chang, C. B., Dunn, K. P., and Willner, D., "Maneuvering Reentry Vehicle Engagement Miss Distance Achievable by Trilateration Radar Tracking," Lincoln Lab. Massachusetts Inst. of Technology, Lexington, MA, Project Rept. RMP-100, Sept. 1976.

[5]Bryson, A. E., Jr., Denham, W. F., and Dreyfus, S. E., "Optimal Programming Problems with Inequality Constraints 1: Necessary Conditions for External Solutions," *AIAA Journal,* Vol. 1, Nov. 1963, pp. 2544–2550.

[6]Stallard, D. V., "Discrete Optimal Terminal Control with Application to Missile Guidance," *IEEE Transactions on Automatic Control,* Vol. AC-18, Aug. 1973, pp. 373–377.

[7]Speyer, J. L., "An Adaptive Terminal Guidance Scheme Based on an Exponential Cost Criterion with Application to Homing Missile Guidance," *IEEE Transactions on Automatic Control,* Vol. AC-21, June 1976, pp. 371–375.

[8]Nazaroff, G. J., "An Optimal Terminal Guidance Law," *IEEE Transactions on Automatic Control,* Vol. AC-21, June 1976, pp. 407–408.

[9]Dowdle, J. R., Gully, S. W., Willsky, A. S., Athans, M., Gendron, R. F., and Cheal, J., "Endgame Guidance Study," ALPHATECH, Inc., Burlington, MA, Rept. TR-141, April 1983.

[10]Gelb, A. and Vander Velde, W. E., *Multiple-Input Describing Functions and Nonlinear Systems Design,* McGraw-Hill, New York, 1968.

[11]Mehra, R. K., Larimore, W., and Ehrich R., "Strapdown Seeker Advanced Guidance for Short Range Air-to-Air Missiles," U.S. Air Force Armament Div., Eglin AFB, FL, AFATL-TR-84-47, May 1984.

[12]Van Trees, H. L., *Detection, Estimation, and Modulation Theory, Part I,* Wiley, New York, 1968.

[13]Taylor, J. H., "The Cramer-Rao Estimation Error Lower Bound Computation for Deterministic Nonlinear Systems," *IEEE Transactions on Automatic Control,* Vol. AC-24, April 1979, pp. 343–345.

[14]Schweppe, F. C., *Uncertain Dynamic Systems,* Prentice-Hall, Englewood Cliffs, NJ, 1973.

[15]Abzug, M. J., "Vector Methods in Homing Guidance," *Journal of Guidance and Control,* Vol. 2, May–June 1979, pp. 253–255.

[16]Riggs, T. L., Jr. and Vergez, P. L., "Advanced Air-to-Air Missile Guidance Using Optimal Control and Estimation," U.S. Air Force Armament Division, Eglin AFB, FL, AFATL-TR-81-56, June 1981.

[17] Looze, D. P., Hsu, J. Y., Grunberg, D., and Dion, D. M., "Investigation of Fundamental Issues in the Use of Acceleration Estimates by Endgame Guidance Laws," ALPHATECH, Inc., Burlington, MA, TR-308, Aug. 1986.